buildings

MDPI

Article

Mechanical Performance and Physico-Chemical Properties of Limestone Calcined Clay Cement (LC3) in Malawi

Innocent Kafodya [1], Debojyoti Basuroy [2], Joseph Mwiti Marangu [3], Grant Kululanga [1], Riccardo Maddalena [4] and Viviana Iris Novelli [4,*]

[1] Civil Engineering Department, Malawi University of Business and Applied Sciences, Blantyre 312225, Malawi; ikafodya@poly.ac.mw (I.K.); gkululanga@poly.ac.mw (G.K.)
[2] Society for Technology and Action for Rural Advancement (TARA), New Delhi 110016, India; dbasuroy@devalt.org
[3] Department of Physical Sciences, Meru University of Science & Technology, Meru 60200, Kenya; jmarangu@must.ac.ke
[4] School of Engineering, Cardiff University, Cardiff CF24 3AA, UK; maddalenar@cardiff.ac.uk
* Correspondence: novelliv@cardiff.ac.uk

Abstract: Malawi is one of the least-developed countries in Sub-Saharan Africa with disaster-prone housing infrastructure characterized by poor construction materials. Therefore, there is a need to provide resilient and cost-effective materials, such as limestone calcined clay cement (LC3). However, the exploitation of LC3 in Malawi is limited due to a lack of mineralogical information about the clays and limestone and related strength and durability when used as a cementitious material. In this study, the strength and physico-chemical properties of LC3 systems with 50% and 40% clinker contents (LC3-50 and LC3-40) were investigated. Cement mortar specimens were prepared at water to cement (w/c) ratios of 0.45, 0.5, and 0.6 with varying calcined clay (CC) to limestone (CC/LS) ratios (1:1, 2:1, and 3:1). The effects of CC/LS ratio on the fresh properties, strength, and durability were investigated. The results showed that specimens with 40% Portland cement replacement levels (LC3-40) exhibited higher standard consistency (up to 45%) than LC3-50, porosity in the range of 8.3–13.3%, and maximum water uptake in the range of 3.8–10.9%. On the other hand, LC3-50 samples offered the highest strength of approximately 40 MPa, complying with requirements for pozzolanic cementitious materials, whereas LC3-40 conforms to the strength requirements for masonry cements. This work shows that LC3 systems can be manufactured with local clays and limestone available in Malawi, and used as a sustainable construction material to mitigate carbon emissions as well as boost the local economy.

Keywords: calcined clay; limestone; cement; hydration; porosity; LC3

Citation: Kafodya, I.; Basuroy, D.; Marangu, J.M.; Kululanga, G.; Maddalena, R.; Novelli, V.I. Mechanical Performance and Physico-Chemical Properties of Limestone Calcined Clay Cement (LC3) in Malawi. *Buildings* **2023**, *13*, 740. https://doi.org/10.3390/buildings13030740

Academic Editor: Antonio Caggiano

Received: 15 February 2023
Revised: 3 March 2023
Accepted: 6 March 2023
Published: 11 March 2023

1. Introduction

Malawi is a developing country in Sub-Saharan Africa. It is situated within the East Africa lift system where natural hazards such as tropical cyclones and earthquakes are common. The prevailing poor socio-economic conditions in Malawi result in poor housing infrastructure, especially in informal settlements [1]. Ordinary Portland Cement (OPC) produced from clinker is commonly used in the Malawi construction industry. The records show that annual cement consumption exceeds 370,000 tons [2]. The poor economic status of the country forces the majority of locals to use mud mortar in place of cement, resulting in weak housing infrastructure that is vulnerable to natural disasters. Statistics from past earthquake events indicate that 4000 households were damaged mainly due to the poor quality of the construction materials [1]. The report of the recent series of tropical cyclones shows that more than 193,558 households were affected and 22,000 households were completely damaged, a situation that called for an improvement in the housing infrastructure in Malawi [3]. Whilst cement is expensive in Malawi, its properties improve

infrastructures' durability and strength and it remains a vital construction material to build resilient housing infrastructures.

For decades cement production has been a major contributor to the global carbon footprint and initiatives have been recommended to reduce carbon dioxide (CO_2) emission and energy consumption in cement production in a quest to combat the impact of climate change as stipulated in the UN Sustainable Development Goal 13 [4–6]. The incorporation of supplementary cementitious materials (SCMs) as a partial replacement for OPC has been shown to produce blended cements with better strength and durability performances than conventional Portland cement [4,7,8]. It is reported that about 20% of SCMs such as fly ash, natural pozzolana, ground granulated blast-furnace slag (GGBS), and limestone are used as additives in cement. However, the quality of fly ash and the availability of GGBS are the major drawbacks in their application for cement production [9]. Other notable alternatives are geopolymers that have high prospects for carbon reduction and resource consumption, however, their practical use is foreseen in the medium to long term [10,11]. Limestone calcined clay cement (LC3) is the recent alternative, which is a ternary blended cement based on the combination of Portland cement clinker with calcined clay and limestone. It can be produced with low-grade clay and dolomite-rich limestone [7]. When kaolinitic clays are calcined at temperatures in the range of 500–800 °C, metakaolin (MK) is obtained, which exhibits excellent pozzolanic reactivity when combined with limestone filler [12–14]. The performance of LC3 is comparable to or better than ordinary Portland cement (OPC) at a clinker factor of 0.5, making it a low-cost and environmentally friendly solution for construction material.

In addition to its environmental benefits, LC3 systems have been shown to be economically viable compared to conventional Portland cement. Joseph et al. performed an economic analysis of the production of LC3 from raw materials locally sourced in India [15,16]. Results showed that LC3 concrete provides a more economical alternative to the rising cost of fly ash, due to its transportation, and better-controlled mineralogical quality. There is low production of fly ash in Malawi since the country does not depend on fossil fuels for power generation, making LC3 production a cost-effective alternative to OPC and other blended cements.

Other researchers studied the effects of limestone calcined clay pozzolana (LCCP) on the engineering properties of mortar and concrete, focusing on variations in initial setting times and compressive strength [17]. They concluded that the induction duration and initial setting time of cement paste reduce with an increased cement replacement level. Higher or similar compressive strength could be registered for all the LCCP blends as compared to ordinary Portland cement. Although these results were insightful, it should be acknowledged that the quality of clay and limestone has a bearing on the performance of LC3 and might be even better for Malawian-based samples.

Ez-zaki et al. (2021) assessed factors that control fresh state properties of limestone-calcined clay cement in comparison with Portland and binary cements, by combining rheological measurements with setting time determination and the evaluation of plastic shrinkage [18]. It was concluded that plastic shrinkage occurs from the mixing to the setting of fresh paste and governs microstructural changes due to settlement and evaporation. Several studies reported that low-grade clays with kaolinite content of about 40% may be used for LC3 with good mechanical and durability performance of concrete [7,16,19,20]. On the other hand, other investigations concluded that calcined clays may increase water demand due to the fineness and large specific surface area of the particles, owing to the amorphous structure of kaolinite that results in a loss in workability [19,21].

The durability properties of cementitious materials are critical for the design of concrete structures. Durability issues of LC3 concrete such as porosity, carbonation, chloride diffusion, and steel reinforcement corrosion have been pursued by various researchers. Dhandapani et al. assessed the pore structure of concrete with LC3, OPC, and fly ash cements using mercury intrusion porosimetry [22,23]. Compared to Portland cement-based binders, it was observed that LC3-based materials offer a much-refined microstructure,

further confirmed by low conductivity results. Khan et al. (2018) focused on addressing issues related to carbonation when calcined clay dosages of 15%, 30%, and 45% at a calcined-clay-to-limestone ratio of 2:1 were used [21]. The results indicated that concrete with LC3 and 15% dosage showed higher carbonation resistance than concrete with OPC. Nguyen et al. (2020) [24] and Rengaraju et al. (2019) [25] evaluated the chloride diffusion resistance of concrete with LC3 using three series of concrete batches. Two dosages with 15% and 20% of the cement were replaced by a mixture of calcined clay and limestone in a ratio of 2:1. The results revealed that the use of LC3 in concrete significantly increases its resistance to chloride diffusion and provides better protection of steel against corrosion.

Pillai et al. (2019) have reported concrete parameters such as chloride diffusion coefficient, aging coefficient, and chloride threshold for cement mixtures containing OPC and blends of OPC with pulverized fuel ash (PFA) or LC3 [26]. The parameters were used to establish the service life of the two construction elements. The results showed that construction with LC3 possesses longer service life with a much smaller carbon footprint.

Although the literature indicates the good performance of LC3-based cementitious materials, there are variations in the properties of raw materials used for various studies. The raw materials are mainly country-specific whose characteristics depend on the geological formations. It is anticipated that Malawian-based raw materials will produce LC3 systems with specific characteristics owing to the unique geological nature of the country.

There are significant quantities of natural raw materials such as limestone and kaolinite clays to produce cost-effective and sustainable limestone calcined clay cement (LC3) in Malawi [2]. The limestone and dolomite resources in Malawi are estimated to be over 800 million tons in the form of metamorphic marble in the southern region. The kaolinite clay and gypsum are estimated to be over 14 million tons and 8000 tons, respectively, in the central region. Irrespective of abundant resources, LC3 production in Malawi is not yet explored due to the unavailability of substantive information about the characteristics of clays and limestone, guidelines on LC3 system formulations, strength, and durability. However, attempts have been made to characterize some clays and limestone in Malawi for potential application in LC3 production [27]. It is therefore imperative to investigate the properties of LC3 with mineral constituents sourced in Malawi in order to establish a potential replacement of OPC to manufacture low-cost, sustainable, durable, and resilient construction. It should be acknowledged that the highest percentage of housing stock in Malawi is unreinforced masonry with fired bricks [28]. LC3 is a potential binder for soil-stabilized blocks that can replace fired bricks thereby promoting environmental conservation. It is anticipated that LC3 production could foster the creation of small to medium business enterprises in the mining sector, which is a pillar in Malawi's Vision 2063 agenda [29].

In this study, the strength and physico-chemical properties of LC3 blends with raw materials sourced in Malawi were investigated. The LC3 constituents were characterized using thermogravimetric (TGA), X-ray fluorescence (XRF), and X-ray diffraction (XRD) analyses. Two types of ternary cement systems namely, LC3-50 (50% clinker content) and LC3-40 (40% clinker content) were investigated. The fresh properties were determined by standard consistency and setting time tests. The strength at 28 days strength was measured at varying calcined clay-to-limestone and water-to-cement ratios. Finally, the porosity of the better-performing LC3 system was determined and a strength-porosity relationship was established.

2. Materials and Methods

2.1. Materials

The raw materials for manufacturing LC3 systems were clay, limestone, clinker, and gypsum. The clay soil was sampled from Lithipe in Central Malawi, (−14.172479, 34.114961). Limestone was obtained from the mining site in Balaka, Southern Malawi (−15.042424, 35.050234). The map showing the location of the raw materials source is shown in Figure 1. Clinker was obtained from a local Lafarge cement manufacturing

distributor in Blantyre, conforming to the international requirements for Portland cement. Natural gypsum was collected from the deposit in the Dowa district located in Central Malawi.

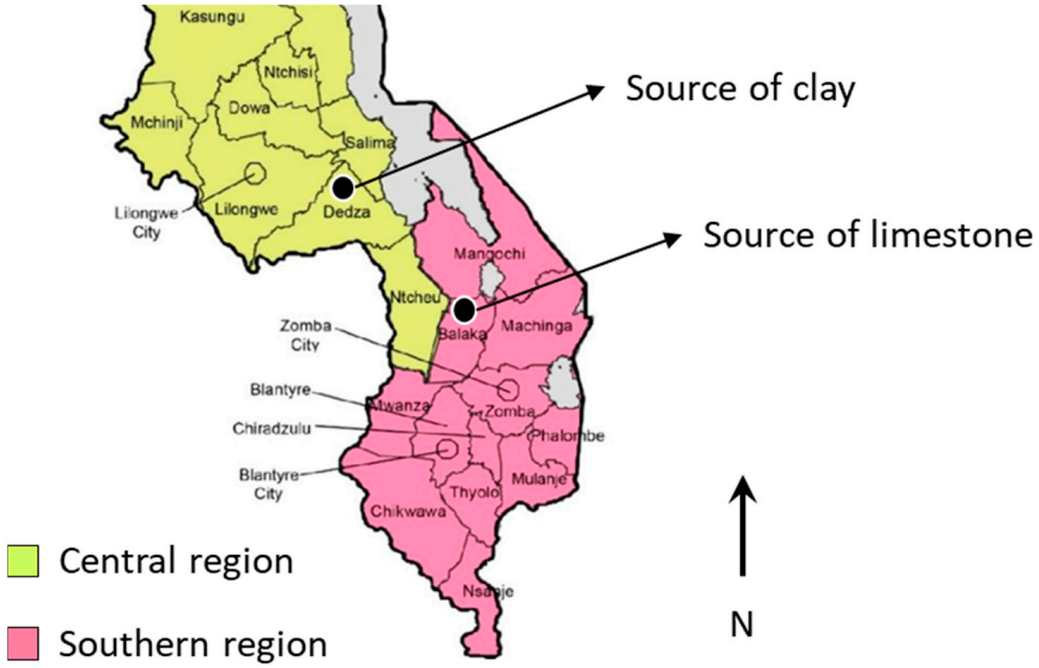

Figure 1. Geographical locations of sampled clay and limestone in Malawi. Image adapted from Maduekwe and de Vries (2019) [30].

2.2. Methods

2.2.1. Materials Preparation

Limestone, gypsum, and clinker were ground separately to produce a fine powder. The clay soil was initially pulverized and sieved using a 75 µm sieve. Only volumes finer than 75 µm were used for preparing LC3 systems. Calcined clay was produced using a static calcination process, where a 50 g clay sample was heated at 800 °C in a muffle furnace for 30 min. The loss on ignition (L.O.I.) index and the mineralogical composition of LC3 constituents obtained by means of X-ray fluorescence (XRF) are shown in Table 1.

Table 1. XRF analysis of LC3 constituents and L.O.I. index.

Compound	Chemical Composition (Oxides, %)				
	Clinker	Clay	Calcined Clay	Limestone	Gypsum
Na_2O	0.03	0.009	0.003	0.003	0.003
MgO	4.00	0.12	0.20	9.20	4.80
Al_2O_3	7.35	29.44	36.03	1.65	1.90
SiO_2	34.07	48.15	46.71	6.45	1.50
P_2O_5	0.36	0.06	0.06	0.034	0.00
SO_3	1.19	0.06	0.83	0.34	52.5
Cl	0.03	0.007	0.004	0.002	0.005
K_2O	0.65	0.3	0.35	0.05	0.01
CaO	52.17	0.44	0.71	47.26	32.01
TiO_2	0.3	0.40	0.43	0.057	0.02
MnO	0.004	0.02	0.022	0.018	0.004
Fe_2O_3	2.58	2.9	3.35	0.61	0.07
L.O.I.	0	18.09	11.30	34.32	7.17

The limestone used sampled in Balaka (Malawi) contained a significant amount of magnesium oxides (MgO) at 9.2%, which might affect the strength development of cement

pastes due to the formation of brucite during hydration [31,32]. The calcination temperature and kaolinite content of clay were determined by means of TGA and XRD analyses, respectively. The results are shown in Figure 2.

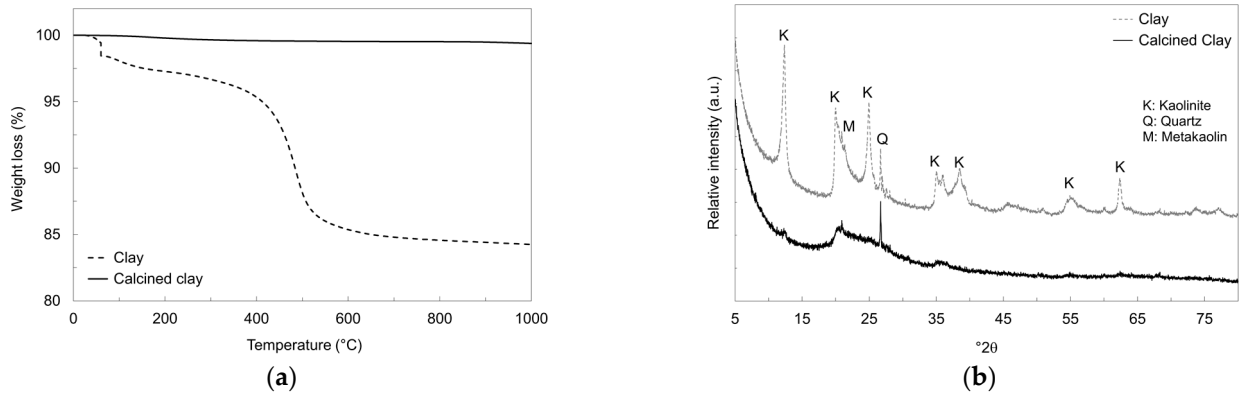

Figure 2. (**a**) TGA profiles and (**b**) XRD patterns of raw clay and calcined clay.

The TGA results showed that dehydroxylation of kaolinite to metakaolin occurred in the region of 400–600 °C with a weight loss of approximately 9%, indicating an initial kaolinite content of 63%. The calcination temperature was therefore determined at 800 ± 10 °C to ensure the full dehydroxylation of kaolinite, in agreement with previous studies [7,33]. The XRD patterns for the raw clay showed the presence of kaolinite as a dominant mineral phase. The peak at around 12° 2θ associated with kaolinite further confirmed high content from TGA analysis, whilst no kaolinite phases are visible in the calcined clay pattern after calcination.

Two ternary cement systems, LC3-50 and LC3-40, were prepared with a Portland cement replacement at 50% and 40% by mass, respectively. For both systems, three series were designed with varying calcined clay to limestone (CC/LS) ratios of, respectively, 1:1, 2:1, and 3:1. For each series, the water to cement (w/c) ratio was kept at 0.45, 0.5, and 0.6. The gypsum content was chosen at 5% by mass in both series to ensure suitable mechanical strength development [19]. The series mix designs are summarized in Table 2.

The workability of the cement systems, and the effect of the calcined clay content, were measured by determining standard consistency, and initial and final setting times, following the methodology reported in ASTM C187 and ASTM C191, respectively [34,35]. The paste for both initial and final setting times was prepared using the predetermined normal consistency of each cement system.

2.2.2. Specimen Preparation for LC3 Mortars

Three mortar prismatic specimens for compressive strength and water absorption rate were measurements were prepared in accordance with BS EN 196-1:2016 using standard sand [36]. After mixing and casting, the specimens were kept in a temperature-controlled environmental chamber at 21 °C and relative humidity of 90% for 24 h. Specimens were then demolded and placed in a water-curing tank for 27 days. After curing, mortar prisms from each cement system and series were air-dried and tested for mechanical strength following the standard BS EN 196-1:2016 [36].

2.2.3. Pore Size Distribution and Electron Microscopy Imaging

Mercury Intrusion Porosimetry (MIP) was used to measure the pore size distribution of the mortar samples cured for 28 days. Prior to MIP measurements, the hydration was halted by isopropanol exchange for three days [37]. The pore diameters were measured in the range between 0.65 mm and 0.003 µm. A micromeritics AutoPore V9600 porosimeter (Micromeritics Instrument Corporation, Norcross—GA, USA) was used. The pressure applied by the porosimeter was in the range of 0–420 MPa with a constant contact angle

of 140°. Scanning electron microscopy (SEM) imaging and chemical analysis was carried out on selected samples using a Zeiss Sigma HD FEG-SEM (Zeiss, Oberkochen, Germany). Secondary electron (SE) imaging and energy dispersive spectroscopy (EDS) X-ray analysis was performed under high vacuum conditions with a beam energy of 20 kV, and a 60 um diameter final aperture, with a resulting beam current of 1.5 nA.

Table 2. Mix design for LC3-50 and LC3-40 series, at varying calcined clay-to-limestone (CC/LS) ratios by mass and water-to-cement (w/c) ratios by mass. The relative content (%wt.) of clinker, calcined clay, limestone, and gypsum is also reported.

LC3-50					
Calcined Clay to Limestone (CC/LS) Ratio	**Clinker %**	**Calcined Clay %**	**Limestone %**	**Gypsum %**	**Water to Cement (w/c) Ratio**
1:1	50.0	22.50	22.50	5.0	0.45
1:1	50.0	22.50	22.50	5.0	0.5
1:1	50.0	22.50	22.50	5.0	0.6
2:1	50.0	30.00	15.00	5.0	0.45
2:1	50.0	30.00	15.00	5.0	0.5
2:1	50.0	30.00	15.00	5.0	0.6
3:1	50.0	33.75	11.25	5.0	0.45
3:1	50.0	33.75	11.25	5.0	0.5
3:1	50.0	33.75	11.25	5.0	0.6
LC3-40					
Calcined Clay to Limestone (CC/LS) Ratio	**Clinker %**	**Calcined Clay %**	**Limestone %**	**Gypsum %**	**Water to Cement (w/c) Ratio**
1:1	40.0	27.50	27.50	5.0	0.45
1:1	40.0	27.50	27.50	5.0	0.5
1:1	40.0	27.50	27.50	5.0	0.6
2:1	40.0	36.67	18.33	5.0	0.45
2:1	40.0	36.67	18.33	5.0	0.5
2:1	40.0	36.67	18.33	5.0	0.6
3:1	40.0	41.25	13.75	5.0	0.45
3:1	40.0	41.25	13.75	5.0	0.5
3:1	40.0	41.25	13.75	5.0	0.6

2.2.4. Specimen Preparation for Water Absorption Measurements

The specimens for water uptake characteristics were prepared in the same manner as those prepared for the compression test in Section 2.2.2. From the water uptake test, two properties were measured, namely the surface rate of water absorption and the saturation water absorption. The specimens were initially oven dried for 24 h at 60 °C. The water absorption rate of absorption was performed following the methodology outlined in ASTM C1403-15 [38] by placing oven-dried specimens into contact with water and the capillary absorption rate was measured after 2 h, 72 h, and 120 h.

3. Results and Discussions

3.1. Effect of Limestone on Calcined Clay Ratio Standard Consistency and Setting Time

The effects of the calcined clay to limestone (CC/LS) ratio on the standard consistency of LC3-50 and LC3-40 are summarized in Figure 3.

The results showed that the standard consistency (%) of both LC3-50 and LC3-40 systems increased with an increasing CC/LS ratio. The standard consistency of LC3-50 varied between 37.5% and 42.5%, whilst LC3-40 ranged between 38.8% and 45%, with consistency values increasingly proportional to the calcined clay content. In comparison, LC3-40 exhibited a standard consistency of 1.9% higher than LC3-50. This is due to the nature of calcined clay, mainly composed of amorphous metakaolin. Amorphous phases provide a large surface area for water absorption due to their disordered arrangement

of molecules that allows penetration and dissolution of the water. Therefore, the higher the metakaolin content, the higher the quantity of water required to achieve cement paste consistency [19,39]. The effect of the (CC/LS) ratio on the setting times is shown in Figure 4.

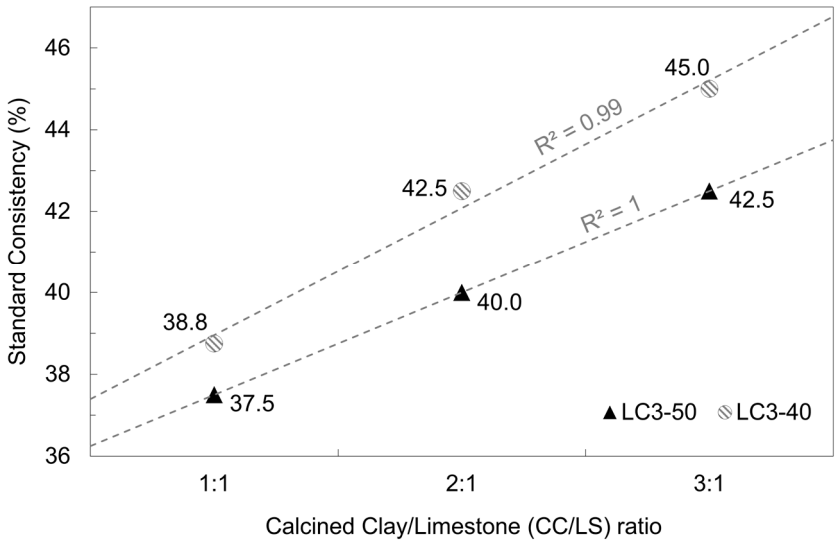

Figure 3. Variation of standard consistency with calcined clay to limestone ratio.

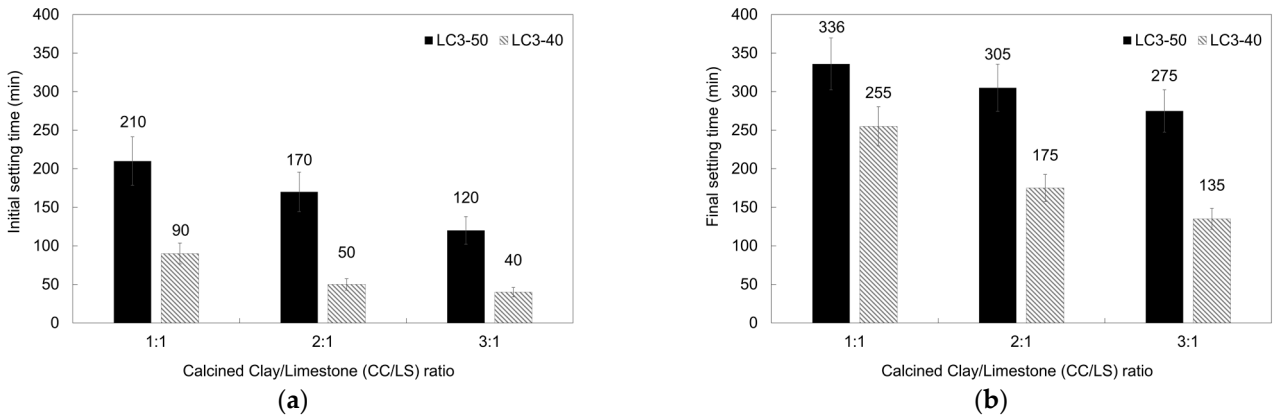

Figure 4. Variation of setting times (**a**) Initial setting time (**b**) final setting time.

Initial and final setting times were reduced with an increase in calcined clay content in both cement systems. LC3-50 showed delayed initial and final setting times compared to LC3-40, with initial setting time varying between 210 min at 1:1 CC/LS ratio and 120 min at 3:1 CC/LS ratio. On the other hand, the initial setting time for LC3-40 varied between 90 min at the 1:1 CC/LS ratio and 40 min at the 3:1 CC/LS ratio. An increase in clinker factor in the cement system from 0.4 to 0.5 resulted in a delayed initial setting time by two-fold. Final setting times showed similar trends with the values of LC3-50 ranging between 336 min at 1:1 CC/LS ratio and 275 min at 3:1 CC/LS ratio. In the case of LC3-40, the final setting time was recorded between 255 min at a 1:1 CC/LS ratio and 135 min at a 3:1 CC/LS ratio. The final setting times for LC3-50 and LC3-40 were reduced by 61 min and 120 min, respectively. Reducing the clinker factor from 0.5 to 0.4 resulted in an accelerated setting time of almost 100 min. BS EN 197-1:2011 recommends initial setting times for conventional cements (strength class 32.5 MPa) should be greater than 75 min, thus all LC3-50 cement systems and LC3-40 at 1:1 CC/LS comply with the required setting time [40]. However, the reduction in setting time could be attributed to a high rate of hydration in the presence of reactive metakaolin in calcined clay, leading to faster calcium silicate hydrates (C-S-H) nucleation that resulted in a build-up of bridges between cement particles [18]. On

the other hand, the delay in setting time with the reduced clinker factor could be attributed to the modifications of the chemical equilibria of the cement in the presence of calcined clay, coupled with lower hydration rate, thus retarding portlandite precipitation and the subsequent setting [18,41,42].

3.2. Compressive Strength and SEM Images of LC3 Systems

The 28 day compressive strength of systems LC3-50 and LC3-40 at varying CC/LS ratios at w/c ratios are shown in Figure 5.

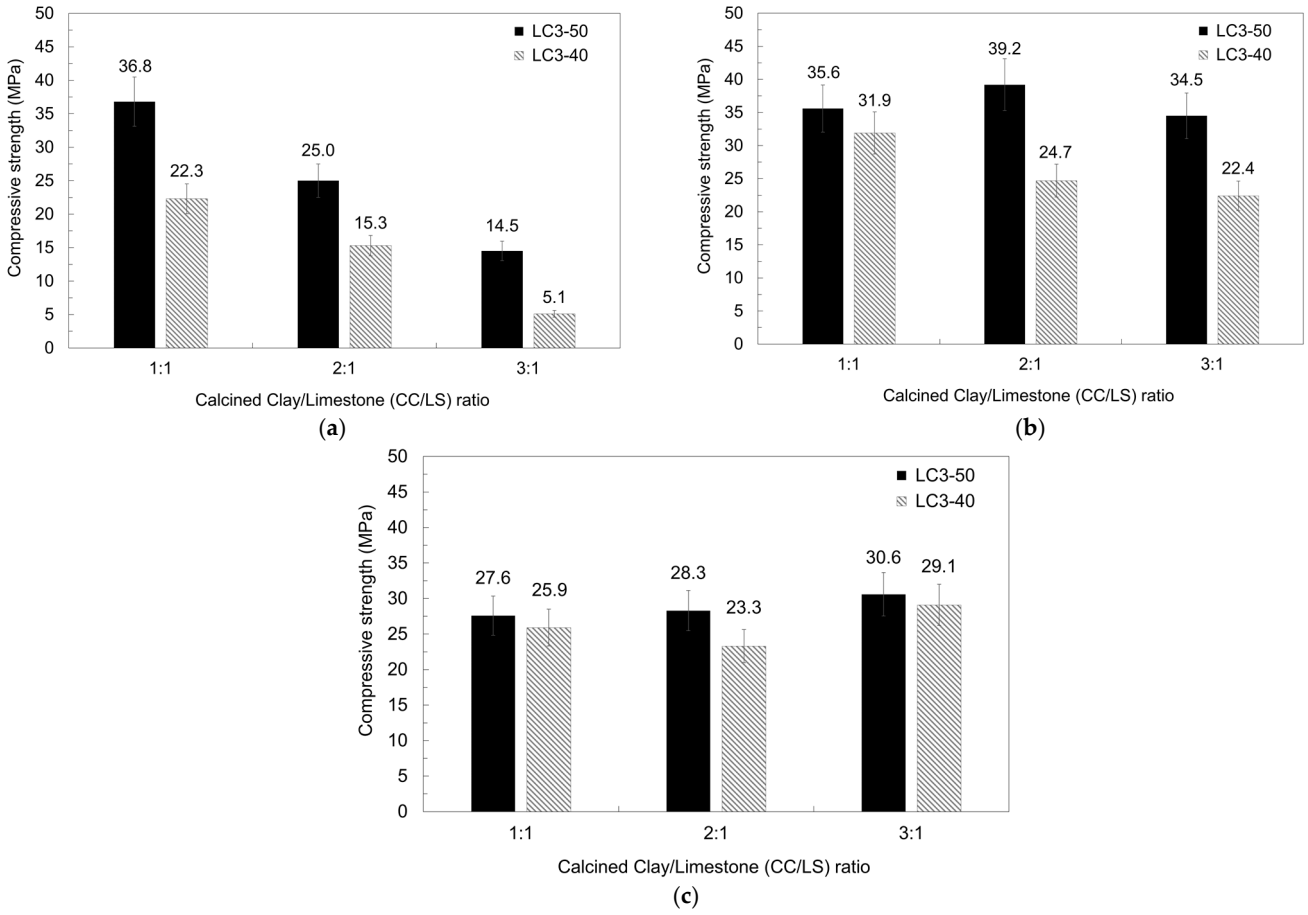

Figure 5. 28-day compressive strength of LC3-50 and LC3-40 at (**a**) 0.45 w/c ratio, (**b**) 0.5 w/c ratio and (**c**) 0.6 w/c ratio.

The compressive strength reduced with an increase in calcined clay content for both LC3-50 and LC3-40 at 0.45 w/c ratio. The maximum compressive strength values of LC3-50 were 36.8 MPa, 39.2 MPa, and 30.6 MPa for 0.45, 0.5, and 0.6 w/c ratio, respectively. For LC3-40, the maximum strength values were 22.3 MPa, 31.9 MPa 29.1 MPa for 0.45, 0.5, and 0.6 w/c ratios, respectively. The lowest strength (5.1 MPa at 0.45 w/c ratio and 3:1 CC/LS ratio) was attributed to the low workability of the cement mixture. Low compaction of the fresh mortar resulted in an increase in the pore volume of hardened mortar and ultimately low strength [43,44]. Additionally, the high calcined clay content and subsequent high pozzolanic reactivity resulted in reduced levels of dissolved portlandite in the liquid phase, inhibiting the full hydration of metakaolin phases and, in turn, hindering the final strength [45]. Segregation of aggregate in the cement mortar due to water in excess of the amount required for hydration is also a possible cause of low-strength development [44,46,47]. LC3-40 was expected to have lower strength than LC3-50 systems due to the reduced initial amount of Portland cement clinker.

According to BS EN 197-1:2011 [40] and BS EN 413-1:2011 [48] specifications, specimens in series LC3-50 with CC/LS ratio of 1:1 complied with the strength requirements for conventional Portland pozzolana cement (PPC) whilst LC3-40 series met the requirements for masonry cement. Furthermore, samples in series LC3-50 with 0.5 w/c ratio also showed the strength requirements for standard Portland cement for all CC/LS ratios. At a w/c ratio of 0.6, for all CC/LS ratios, both LC3-50 and LC3-40 series complied with masonry cement strength requirements. Based on the standard strength requirements for PPC, LC3-50 at 0.5 w/c ratios can potentially replace standard Portland cement [27].

3.3. Pore Size Distribution and SEM Images

Based on the strong performance, the pore size distribution of selected samples from the LC3-50 system series was measured, and the results are shown in Figure 6.

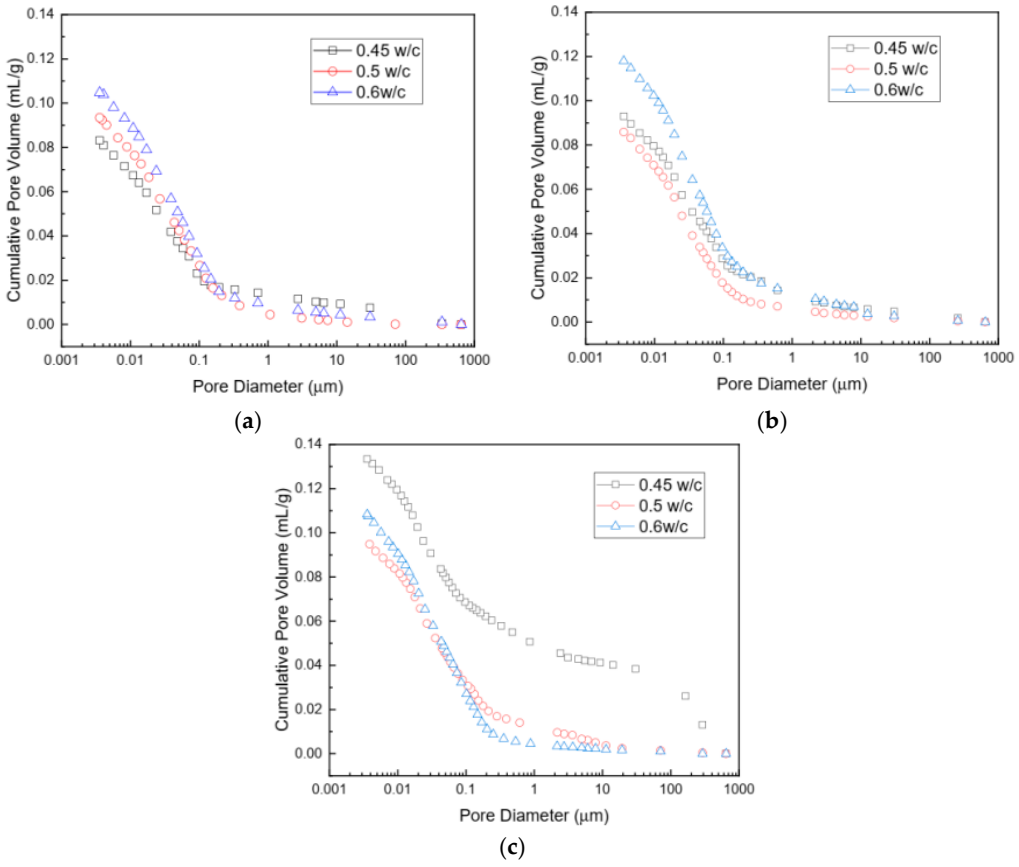

Figure 6. Pore size distribution of LC3-50 system at (**a**) 1:1 CC/L (**b**) 2:1 CC/L (**c**) 3:1 CC/L.

The cumulative pore volume ranges between approximately 0.08 and 0.13 mL/g for all LC3-50 series. Samples at a w/c ratio of 0.6 showed the highest cumulative pore volume for series at CC/LS ratios of 1:1 and 2:1. However, at the highest calcined clay content (3:1 CC/LS) samples at a w/c ratio of 0.45 showed a higher cumulative pore volume, suggesting that the water-to-cement ratio influences the hardened pore structure [49]. This effect is in fact more evident in the pore size region of capillary pores; the higher the w/c ratios for 1:1 CC/LS and 2:1 CC/LS, the larger the pores. All cumulative pore volume curves present a generalized lognormal with sigmoidal distribution except for samples at a w/c ratio of 0.45 with the highest clay content (3:1 CC/LS), which exhibits two inflection points. This is indicative of two-phased volume intrusion; the first phase could be due to an intrusion into the micro-cracks or air pockets at the sand-cement interfaces, whereas the second phase could be attributed to intrusions into interconnected pores of the hydrated

cement. The critical pore entry sizes at various w/c ratios and CC/LS ratios are shown in Figure 7.

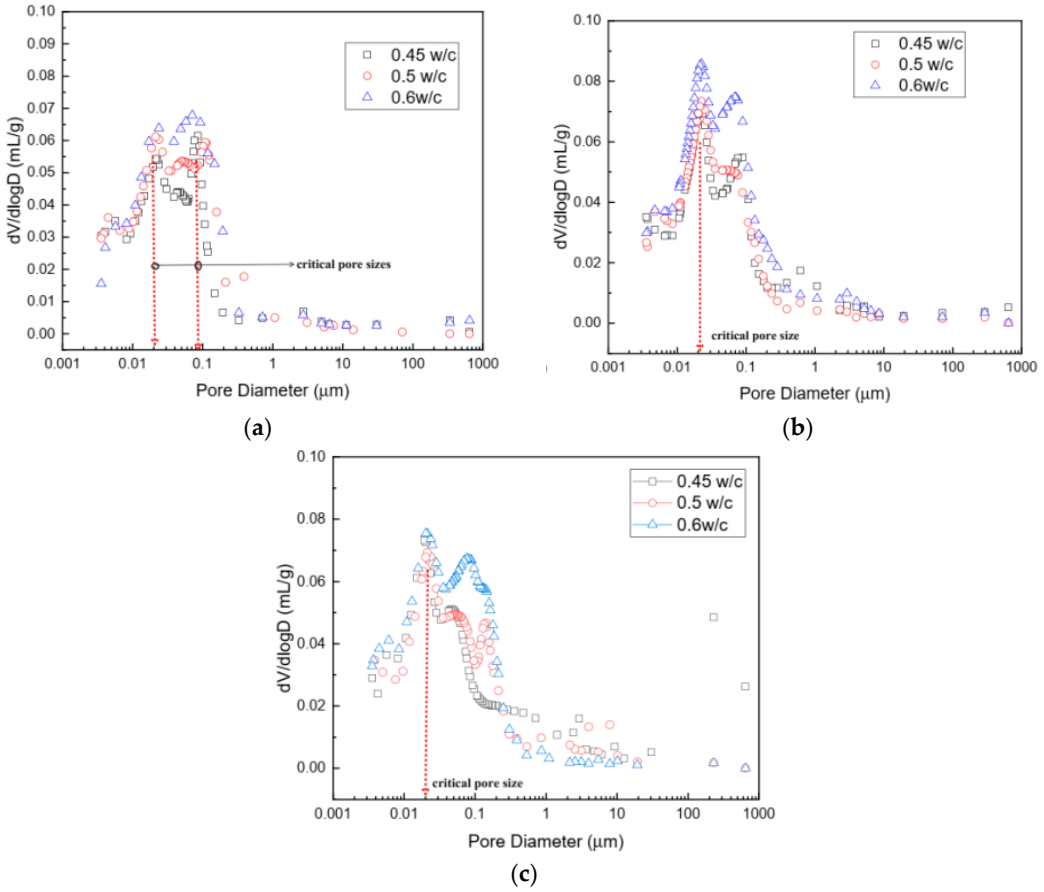

Figure 7. Differential intruded volume for LC3-50 system at (**a**) 1:1 CC/LS (**b**) 2:1 CC/LS (**c**) 3:1 CC/LS.

The bimodal differential intruded volume curves are shown for all mortar series in the LC3-50 system. The curves indicate the coexistence of both coarse and fine pores in the hardened mortar microstructure. The critical pore entry sizes range between 0.019 μm and 0.08 μm and the total porosity is between 2.6% and 10.6%, respectively. The values are consistent with the findings reported in previous work [49–51].

The morphological images of LC3-50 that exhibited superior strength properties are shown in Figure 8. The SEM images showed variations in the composition of elements from different points of analysis. For site 1 (2:1 CC/LS series at w/c ratio of 0.45), the three elements with relatively high percentages are O, Ca, and Si, suggesting the presence of calcium silicate hydrate (C-S-H) phases. For site 2 (2:1 CC/LS series at w/c ratio of 0.5), the dominant elements (composition > 10%) are O, Si, C, and Ca indicating the presence of C-S-H phases and carbo-aluminates. The latter contributes to space-filling, thus reducing porosity, and resulting in enhanced overall strength. The positive effects of carbo-aluminates precipitation on the mechanical properties have been reported elsewhere [41,52,53], confirming the higher compressive strength exhibited by LC3-50 systems at a 2:1 CC/LS ratio with w/c ratio of 0.5 (approximately 40 MPa). For site 3 (3:1 CC/LS series at w/c ratio of 0.6), the dominant elements are O, Fe, Si, C, and Ca. The site is considered to have intermixing of compounds, namely C-S-H, tetra-calcium ferrite (C4F) and carbo-aluminates.

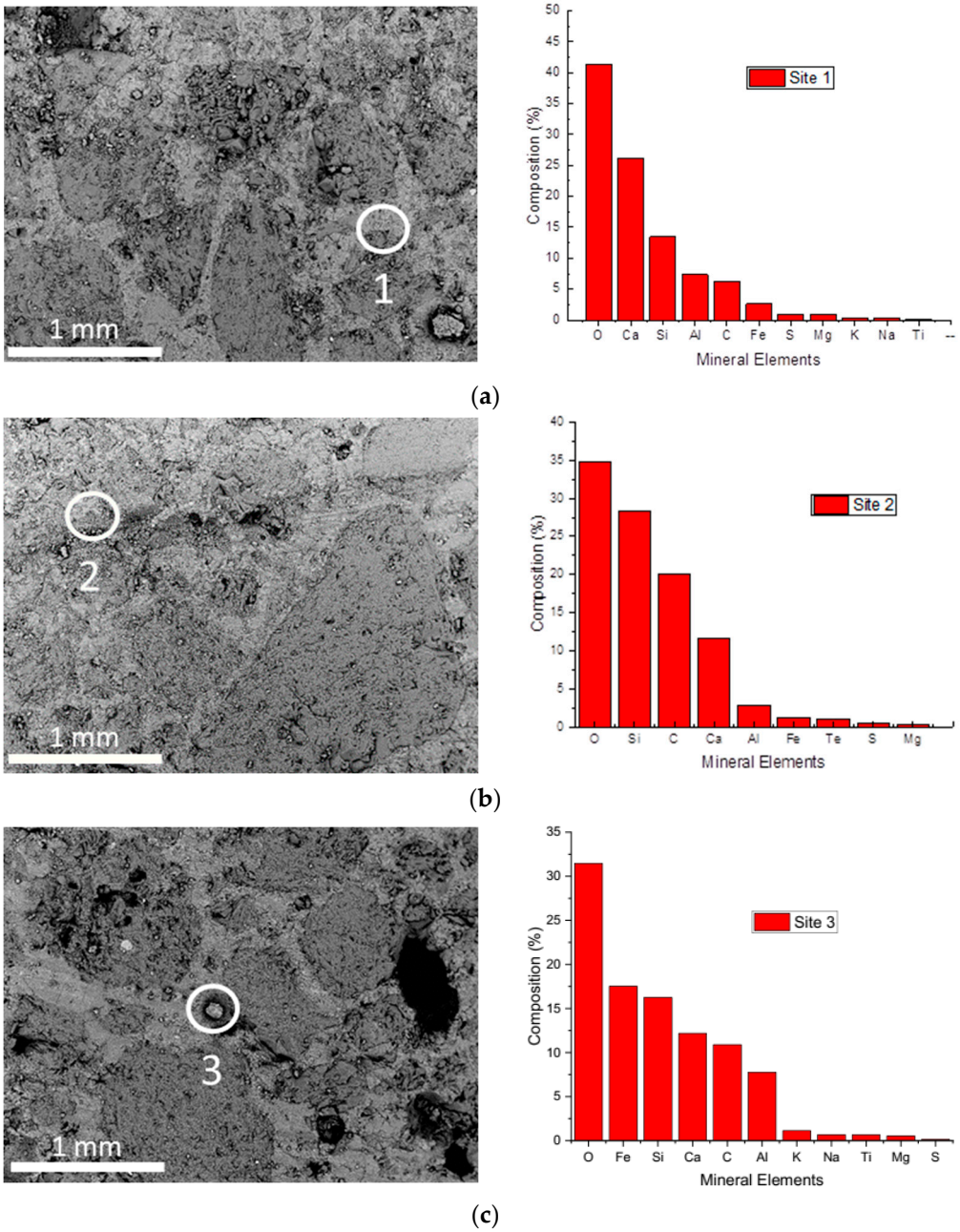

Figure 8. Selected SEM images and chemical mapping for LC3-50 system series with the highest strength. (**a**) 2:1 CC/LS ratio at w/c ratio of 0.45; (**b**) 2:1 CC/LS ratio at w/c ratio of 0.5; and (**c**) 2:1 CC/LS ratio at w/c ratio of 0.6.

The Bogue–Lerch strength values as reported in Beaudoin and Odler (2019) ranks tetra-calcium alumino-ferrite (C4AF) phases as lowest during the early stages of hydration [54]. Hence, the lower strength exhibited by LC3-50 with 3:1 CC/LS at a w/c ratio of 0.6 (approximately 31 MPa) could be attributed to the formation of C4AF, counteracting the strength-enhancing effects of carbo aluminates phases. The microstructural development of LC3 systems from 21 randomly selected points of the cement mortar using SEM-EDS is presented by the Si/Ca and Al/Ca ratios shown in Figure 9. The scatter of the composition is relatively high, indicating a non-uniform consumption of silicate and alumina in calcium aluminate silicate hydrate (C-A-S-H) phases and also greater inter-mixing of the aluminates with the final product, as reported in literature [55,56].

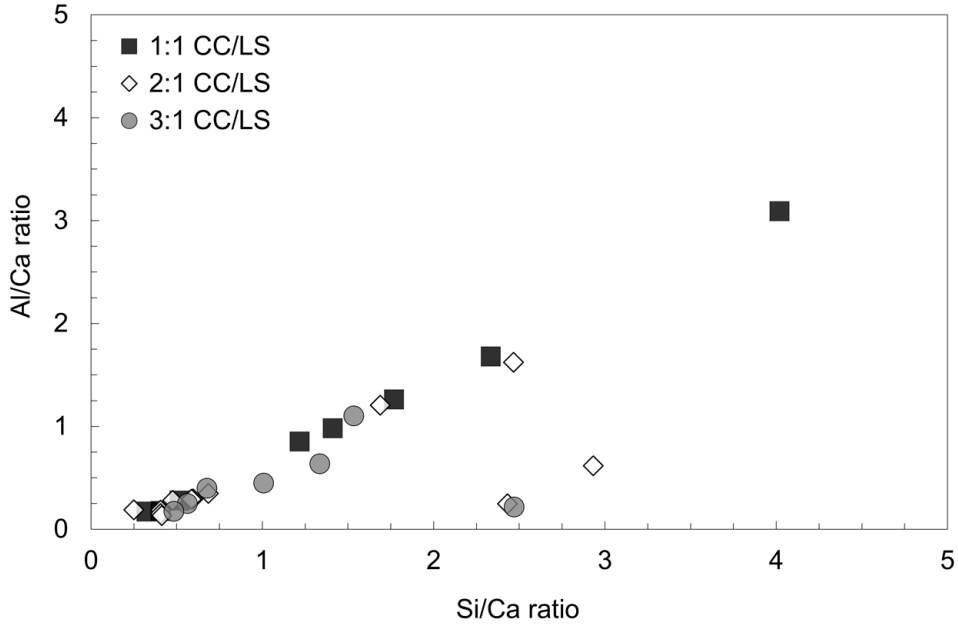

Figure 9. Si/Ca vs. Al/Ca scatter plot ratio values for LC3-50 samples with higher strength.

3.4. Relationship between Compressive Strength and Porosity

Several models have been proposed to predict the strength of the cement mortar as a function of its porosity [57–61], summarize in Table 3.

Table 3. Prediction models of porous materials.

Model	Equation	Parameters	Material
Balshin [57]	$\sigma = \sigma_o(1-p)^b$	[1] σ_o, b	Ceramic materials
Ryshkevitch [58]	$\sigma = \sigma_o e^{-kp}$	σ_o, k	Mortar containing Al_2O_3 and ZrO_2
Schiller [59]	$\sigma = n\ In\left(\frac{p_o}{p}\right)$	N	Sulfate plasters
Hasselman [60]	$\sigma = \sigma_o - cp$	σ_o, c	Refractory materials
Xudong-Chen modified Zheng model [61]	$\sigma = \sigma_o\left[\left(\frac{p_c-p}{p_c}\right)^m\left(1-p^{\frac{2}{3}}\right)\right]^{0.5}$	[2] $\sigma_o,\ p_c, m$	Ordinary Portland cement mortar

[1] σ_o is Strength at zero porosity, [2] p_c is the percolation porosity at failure threshold.

The regression analysis of all LC3-50 system series irrespective of their w/c ratios and CC/LS ratios were used in prediction models, and results are shown in Figure 10a. A linear relationship between compressive strength and total porosity, obtained from MIP measurements, has been found, with a coefficient of correlation of 0.66. This indicates that the strength of the cementitious materials is influenced by porosity. The regression analysis was then compared with the prediction models (Figure 10b). Whilst the measured strength values vary considerably as opposed to the predicted ones, the models however were developed for specific cementitious materials, and the effects of the water-cement ratio are not incorporated in the model parameters. The strength is also dependent on other factors, such as age, curing conditions, and mineralogical composition of the starting materials, as demonstrated in the previous section. Therefore, adequately choosing model parameters must be carefully considered for the prediction of the strength of cement-based materials. However, the general trends are consistent for both predicted and measured values.

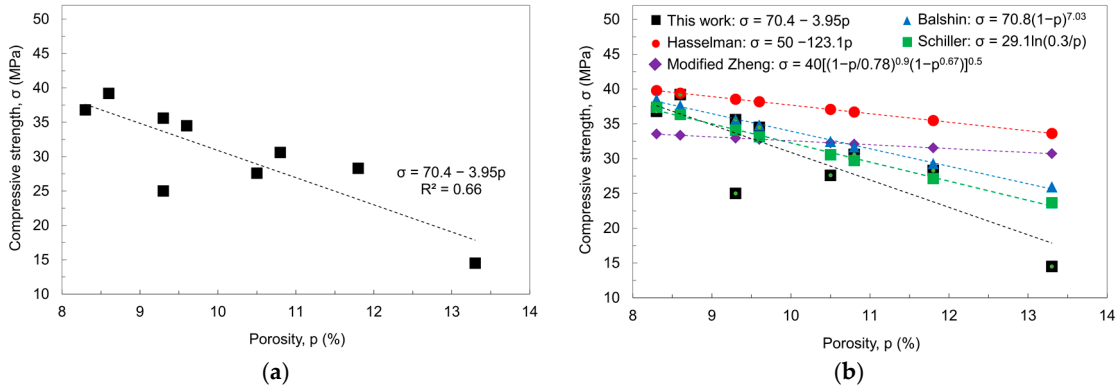

Figure 10. Relationship between compressive strength and total porosity (**a**) for experimental data; and (**b**) comparison with values obtained from strength prediction models.

3.5. Capillary Water Absorption

The capillary surface water absorption test was performed on selected specimens at a w/c ratio of 0.5, based on the compressive strength results. The results for both LC3 systems (LC3-50 and LC3-40) are shown in Figure 11. Specimens exhibited a high initial water absorption rate (0 to 60 min) for both LC3-50 and LC3-40 system series. After 24 h, LC3-50 samples with 1:1, 2:1, and 3:1 CC/LS ratios showed rates of surface water absorption of 66.07 g/100 cm^2, 67.85 g/100 cm^2, and 74.92 g/100 cm^2, respectively.

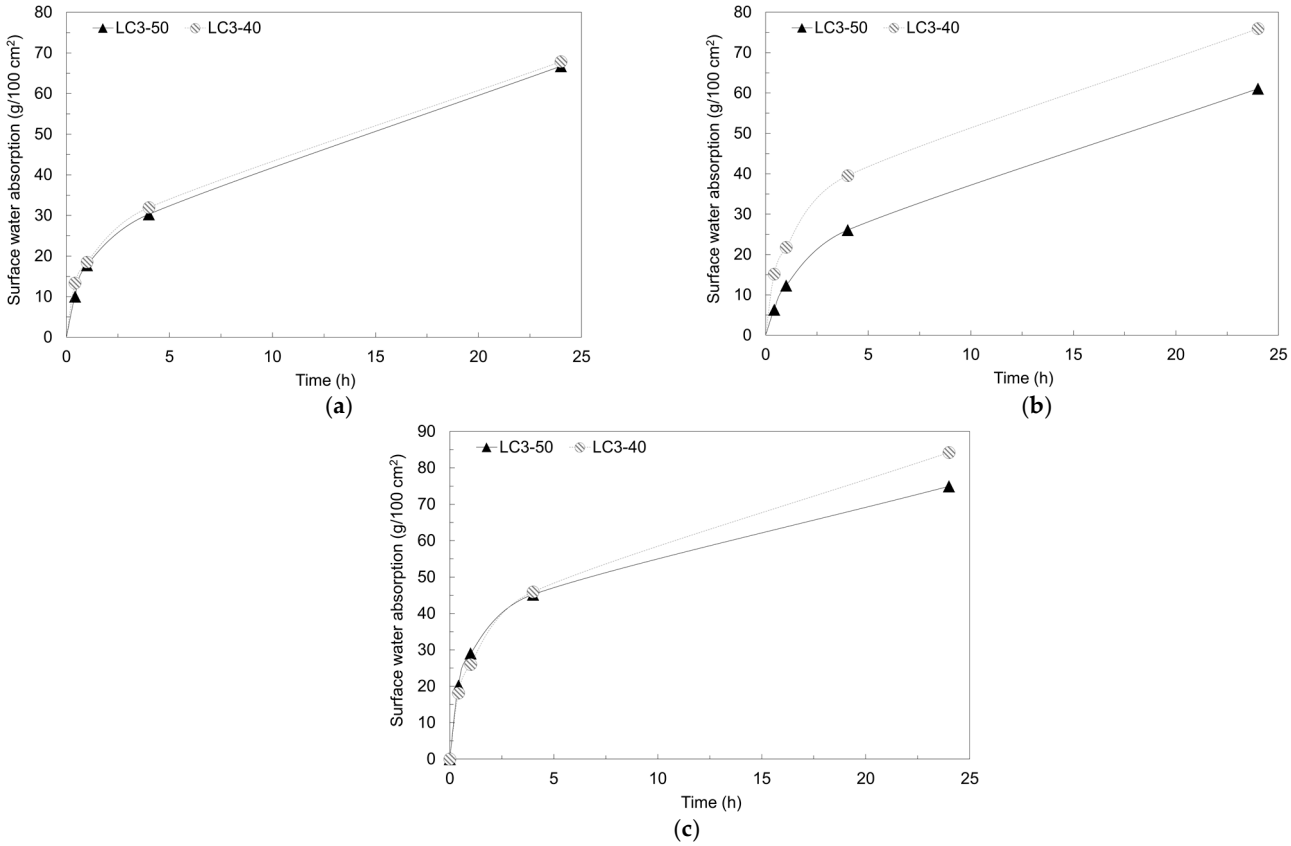

Figure 11. Surface water absorption rates of LC3 systems at (**a**) 1:1 CC/LS ratio (**b**) 2:1 CC/LS ratio (**c**) 3:1 CC/LS ratio.

On the other hand, LC3-40 with 1:1, 2:1, and 3:1 CC/LS ratios indicated a rate of surface water absorption after 24 h of 66.84 g/100 cm^2, 75.93 g/100 cm^2, and 80.23 g/100 cm^2,

respectively, slightly higher than specimens in LC3-50 series. The reduced water absorption for LC3-50 specimens could be due to the higher rate of hydration, resulting in a refined pore structure [62,63]. Conversely, an increased surface water absorption for samples with the higher calcined clay content for both LC3 systems is attributed to a higher amount of unreacted metakaolin; its large surface area favors water uptake [18,19]. The maximum water uptake values (%) after 24 h for the two LC3 systems at a w/c ratio of 0.5 are shown in Figure 12.

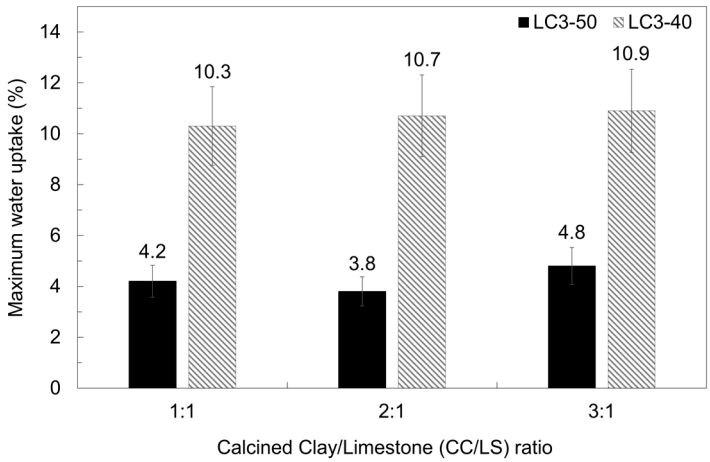

Figure 12. Maximum water uptake at 24 h for the LC3-50 and LC3-40 systems at a w/c ratio of 0.5 and varying calcined clay/limestone (CC/LS) ratios.

Both LC3 systems showed similar values of maximum water uptake, approximately an average of 4.0% and 10.5% for the LC3-50 and LC3-40 series, respectively. The higher absorption for LC3-40 is proportional to the total porosity at critical pore entry sizes. Thus, the higher water uptake is attributed to the combined effect of the high volume of pores, otherwise filled with hydration products in the LC3-50 series, and the amorphous nature of the unreacted metakaolin. Higher water uptake might also facilitate chloride transport in cement mortar, a phenomenon that affects its long-term durability.

4. Conclusions

In this study, the strength and physico-chemical properties of LC3 systems in Malawi were investigated. Cement mortar specimens were prepared at water-to-cement (w/c) ratios of 0.45, 0.5, and 0.6 and calcined clay-to-limestone (CC/LS) ratios of 1:1, 2:1, and 3:1, respectively. The effects of (CC/LS) ratios on standard consistency and setting time, and the effects of w/c and CC/LS ratios on compressive strength and porosity were studied. The results presented in this work allowed for the following conclusions to be drawn:

1. Increasing the calcined clay to limestone ratio resulted in an increased standard consistency of LC3-50 specimens, varying between 37.5% at 1:1 CC/LS ratio and 42.5% at 3:1 CC/LS ratio whilst for LC3-40 ranged between 38.75% at 1:1 CC/LS ratio and 45% at 3:1 CC/LS ratio. This is attributed to an increased amount of amorphous metakaolin in the clay-rich systems, implying that LC3-40 samples require more water than LC3-50 to achieve suitable workability for maximum hydration.
2. LC3-50 samples showed delayed initial and final setting times compared to those in LC3-40. The lower clinker factor and high calcined clay content in the LC3 systems are associated with accelerated setting time. Conversely, the presence of more reactive phases such as metakaolin is responsible for the accelerated setting time.
3. Both LC3 systems complied with the strength requirements outlined in international standards. LC3-50 samples with a CC/LS ratio of 2:1 can achieve strength values comparable with standard Portland Pozzolana Cement, whilst the strength of the LC3-40 system is comparable with one of the masonry cements. It is therefore recommended

to use LC3-50 systems in order to realize a significant reduction in carbon footprint with acceptable strength.

4. The critical pore entry sizes of LC3-50 systems at w/c of 0.45, 0.5, and 0.6 range between 0.019 μm and 0.08 μm with total porosity values between 2.6% and 10.6%, indicating a well-refined microstructure.
5. Specimens in the LC3-50 system with high calcined clay content (3:1 CC/LS ratio) and low w/c ratio (0.45) exhibited a bimodal pore distribution due to the coexistence of air pockets and hydrated cement compounds in the microstructure.
6. LC3-50 specimens showed values of maximum surface water absorption up to 60% lower than LC3-40, in line with porosity measurements.
7. The LC3-50 series provides a better environmental performance; the amount of CO_2 emission is expected to reduce by almost 50% owing to the reduced amount of clinker required to produce LC3-50.

Based on the findings abovementioned, further work will be conducted on LC3-50 systems, focusing on their microstructure development and heath of hydration, and the influence of accelerated aging and damage on the mineralogical composition and overall durability.

Author Contributions: Conceptualization, I.K. and V.I.N.; methodology, I.K. and D.B.; validation, formal analysis, I.K., D.B., G.K. and V.I.N.; investigation, I.K. and D.B.; writing—original draft preparation, I.K. and D.B.; writing—review and editing, I.K., D.B., V.I.N., J.M.M. and R.M.; supervision, I.K.; project administration, I.K. and V.I.N.; funding acquisition, V.I.N. All authors have read and agreed to the published version of the manuscript.

Funding: This work was funded by the HEFCW-GCRF via Cardiff University (HEFCW GCRF Fellowship Award: Limestone Calcined Clay Cement: a low-cost construction material to realize a resilient and sustainable built environment in Malawi). The APC was funded by Cardiff University.

Data Availability Statement: Data associated with the findings presented in this work are available at the Cardiff University data repository under http://doi.org/10.17035/d.2023.0244558110.

Acknowledgments: The authors wish to acknowledge: Duncan Muir, School of Earth and Environmental Sciences, Cardiff University, UK for the support with the SEM images, and Julian Steer, School of Engineering, Cardiff University, UK for the support in acquiring thermogravimetric data.

Conflicts of Interest: The authors declare no conflict of interest.

References

1. Novelli, V.I.; De Risi, R.; Ngoma, I.; Kafodya, I.; Kloukinas, P.; Macdonald, J.; Goda, K. Fragility curves for non-engineered masonry buildings in developing countries derived from real data based on structural surveys and laboratory tests. *Soft Comput.* **2021**, *25*, 6113–6138. [CrossRef]
2. Technology and Action for Rural Advancement. *Analysis of Raw Materials and Assessment of the Reactivity of China Clay from Malawi for LC3 Application*; Technology and Action for Rural Advancement: New Delhi, India, 2016.
3. UNICEF. *Malawi Tropical Storm Ana Situation Report*; UNICEF: New York, NY, USA, 2022.
4. Tironi, A.; Scian, A.N.; Irassar, E.F. Blended Cements with Limestone Filler and Kaolinitic Calcined Clay: Filler and Pozzolanic Effects. *J. Mater. Civ. Eng.* **2017**, *29*, 1–8. [CrossRef]
5. Díaz, Y.C.; Berriel, S.S.; Heierli, U.; Favier, A.R.; Machado IR, S.; Scrivener, K.L.; Hernández, J.F.M.; Habert, G. Limestone calcined clay cement as a low-carbon solution to meet expanding cement demand in emerging economies. *Dev. Eng.* **2016**, *2*, 82–91. [CrossRef]
6. Miller, S.A. Supplementary cementitious materials to mitigate greenhouse gas emissions from concrete: Can there be too much of a good thing? *J. Clean Prod.* **2018**, *178*, 587–598. [CrossRef]
7. Scrivener, K.; Martirena, F.; Bishnoi, S.; Maity, S. Calcined clay limestone cements (LC3). *Cem. Concr. Res.* **2018**, *114*, 49–56. [CrossRef]
8. Yang, K.H.; Jung, Y.B.; Cho, M.S.; Tae, S.H. Effect of supplementary cementitious materials on reduction of CO_2 emissions from concrete. *J. Clean. Prod.* **2015**, *103*, 774–783. [CrossRef]
9. Akindahunsi, A.A.; Avet, F.; Scrivener, K. The Influence of some calcined clays from Nigeria as clinker substitute in cementitious systems. *Case Stud. Constr. Mater.* **2020**, *13*, e00443. [CrossRef]
10. McLellan, B.C.; Williams, R.P.; Lay, J.; Van Riessen, A.; Corder, G.D. Costs and carbon emissions for geopolymer pastes in comparison to ordinary portland cement. *J. Clean. Prod.* **2011**, *19*, 1080–1090. [CrossRef]

11. Habert, G.; De Lacaillerie JD, E.; Roussel, N. An environmental evaluation of geopolymer based concrete production: Reviewing current research trends. *J. Clean. Prod.* **2011**, *19*, 1229–1238. [CrossRef]
12. Scrivener, K.L. Options for the future of cement. *Indian Concr. J.* **2014**, *88*, 11–21.
13. Tironi, A.; Trezza, M.A.; Scian, A.N.; Irassar, E.F. Kaolinitic calcined clays: Factors affecting its performance as pozzolans. *Constr. Build Mater.* **2012**, *28*, 276–281. [CrossRef]
14. Schulze, S.E.; Rickert, J. Suitability of natural calcined clays as supplementary cementitious material. *Cem. Concr. Compos.* **2019**, *95*, 92–97. [CrossRef]
15. Joseph, S.; Joseph, A.M.; Bishnoi, S. Economic Implications of Limestone Clinker Calcined Clay Cement (LC3) in India. In *Calcined Clays for Sustainable Concrete*; Scrivener, K.L., Favier, A.R., Eds.; RILEM: Marne, France, 2015. [CrossRef]
16. Joseph, S.; Bishnoi, S.; Maity, S. An economic analysis of the production of limestone calcined clay cement in India. *Indian Concr. J.* **2016**, *90*, 22–27.
17. Shah, V.; Parashar, A.; Mishra, G.; Medepalli, S.; Krishnan, S.; Bishnoi, S. Influence of cement replacement by limestone calcined clay pozzolan on the engineering properties of mortar and concrete. *Adv. Cem. Res.* **2020**, *32*, 101–111. [CrossRef]
18. Ez-Zaki, H.; Marangu, J.M.; Bellotto, M.; Dalconi, M.C.; Artioli, G.; Valentini, L. A fresh view on limestone calcined clay cement (LC3) pastes. *Materials* **2021**, *14*, 3037. [CrossRef]
19. Sharma, M.; Bishnoi, S.; Martirena, F.; Scrivener, K. Limestone calcined clay cement and concrete: A state-of-the-art review. *Cem. Concr. Res.* **2021**, *149*, 106564. [CrossRef]
20. Nair, N.; Haneefa, K.M.; Santhanam, M.; Gettu, R. A study on fresh properties of limestone calcined clay blended cementitious systems. *Constr. Build Mater.* **2020**, *254*, 119326. [CrossRef]
21. Khan, M.S.H.; Nguyen, Q.D.; Castel, A. Carbonation of Limestone Calcined Clay Cement Concrete. In *Calcined Clays for Sustainable Concrete*; Scrivener, K.L., Favier, A.R., Eds.; RILEM: Marne, France, 2015.
22. Dhandapani, Y.; Santhanam, M. Assessment of pore structure evolution in the limestone calcined clay cementitious system and its implications for performance. *Cem. Concr. Compos.* **2017**, *84*, 36–47. [CrossRef]
23. Dhandapani, Y.; Vignesh, K.; Raja, T.; Santhanam, M. Development of the Microstructure in LC3 Systems and Its Effect on Concrete Properties. In *Calcined Clays for Sustainable Concrete*; Scrivener, K.L., Favier, A.R., Eds.; RILEM: Marne, France, 2015.
24. Nguyen, Q.D.; Castel, A. Reinforcement corrosion in limestone flash calcined clay cement-based concrete. *Cem. Concr. Res.* **2020**, *132*, 106051. [CrossRef]
25. Rengaraju, S.; Neelakantan, L.; Pillai, R.G. Investigation on the polarization resistance of steel embedded in highly resistive cementitious systems—An attempt and challenges. *Electrochim. Acta* **2019**, *308*, 131–141. [CrossRef]
26. Pillai, R.G.; Gettu, R.; Santhanam, M.; Rengaraju, S.; Dhandapani, Y.; Rathnarajan, S.; Basavaraj, A.S. Service life and life cycle assessment of reinforced concrete systems with limestone calcined clay cement (LC3). *Cem. Concr. Res.* **2019**, *118*, 111–119. [CrossRef]
27. Kafodya, I.; Novelli, V. Strength properties of Limestone Calcined Clay Cement (LC3) in Malawi. In Proceedings of the Resilient Materials 4 Life (RM4L2020) International Conference, Wales, UK, 20–22 September 2021.
28. Kloukinas, P.; Novelli, V.; Kafodya, I.; Ngoma, I.; Macdonald, J.; Goda, K. *A Building Classification Scheme of Housing Stock in Malawi for Earthquake Risk Assessment*; Springer: Berlin/Heidelberg, Germany, 2020; Volume 35. [CrossRef]
29. Government of Malawi. *Malawi 2063, Malawi 's Vision. An Inclusively Wealthy and Self-Reliant Nation*; Government of Malawi: Lilongwe, Malawi, 2020; pp. 1–92.
30. Maduekwe, E.; de Vries, W.T. Random spatial and systematic random sampling approach to development survey data: Evidence from field application in Malawi. *Sustainability* **2019**, *11*, 6899. [CrossRef]
31. Wang, L.; Lu, X.; Liu, L.; Xiao, J.; Zhang, G.; Guo, F.; Li, L. Influence of MgO on the Hydration and Shrinkage Behavior of Low Heat Portland Cement-Based Materials via Pore Structural and Fractal Analysis. *Fractal Fract.* **2022**, *6*, 40. [CrossRef]
32. Gonçalves, T.; Silva, R.V.; De Brito, J.; Fernández, J.M.; Esquinas, A.R. Hydration of reactive MgO as partial cement replacement and its influence on the macroperformance of cementitious mortars. *Adv. Mater. Sci. Eng.* **2019**, *2019*, 1–12. [CrossRef]
33. Avet, F.; Li, X.; Scrivener, K. Determination of the amount of reacted metakaolin in calcined clay blends. *Cem. Concr. Res.* **2018**, *106*, 40–48. [CrossRef]
34. *ASTM C187-16*; Standard Test Method for Amount of Water Required for Normal Consistency of Hydraulic Cement Paste. ASTM: West Conshohocken, PA, USA, 2016.
35. *ASTM C191-21*; Standard Test Methods for Time of Setting of Hydraulic Cement by Vicat Needle. ASTM: West Conshohocken, PA, USA, 2021.
36. *BS EN 196-1:2016*; British Standard Methods of Testing Cement—Determination of Strength. BSI: London, UK, 2016.
37. Zhang, J.; Scherer, G.W. Comparison of methods for arresting hydration of cement. *Cem. Concr. Res.* **2011**, *41*, 1024–1036. [CrossRef]
38. *ASTM C1403-15*; Standard Test Method for Rate of Water Absorption of Masonry Mortars. ASTM: West Conshohocken, PA, USA, 2015.
39. El-Diadamony, H.; Amer, A.A.; Sokkary, T.M.; El-Hoseny, S. Hydration and characteristics of metakaolin pozzolanic cement pastes. *HBRC J.* **2018**, *14*, 150–158. [CrossRef]
40. *BS EN 197-1:2011*; Composition, Specifications and Conformity Criteria for Common Cements. BSI: London, UK, 2011.
41. Antoni, M.; Rossen, J.; Martirena, F.; Scrivener, K. Cement substitution by a combination of metakaolin and limestone. *Cem. Concr. Res.* **2012**, *42*, 1579–1589. [CrossRef]

42. Cao, Y.; Wang, Y.; Zhang, Z.; Ma, Y.; Wang, H. Recent progress of utilization of activated kaolinitic clay in cementitious construction materials. *Compos. B Eng.* **2021**, *211*, 108636. [CrossRef]
43. Marangu, J.M. Physico-chemical properties of Kenyan made calcined Clay -Limestone cement (LC3). *Case Stud. Constr. Mater.* **2020**, *12*, e00333. [CrossRef]
44. Chan, N.; Young-Rojanschi, C.; Li, S. Effect of water-to-cement ratio and curing method on the strength, shrinkage and slump of the biosand filter concrete body. *Water Sci. Technol.* **2018**, *77*, 1744–1750. [CrossRef]
45. Aramburo, C.H.; Pedrajas, C.; Talero, R. Portland cements with high content of calcined clay: Mechanical strength behaviour and sulfate durability. *Materials* **2020**, *13*, 4206. [CrossRef]
46. Zunino, F.; Martinera, F.; Scrivener, K.L. Limestone Calcined Clay Cements (LC3). *ACI Mater J.* **2021**, *118*, 49–60.
47. Jaskulski, R.; Jóźwiak-Niedźwiedzka, D.; Yakymechko, Y. Calcined clay as supplementary cementitious material. *Materials* **2020**, *13*, 4734. [CrossRef]
48. *BS EN 413-1:2011*; Masonry Cement Composition, Specification and Conformity Criteria. BSI: London, UK, 2011.
49. Chen, X.; Wu, S. Influence of water-to-cement ratio and curing period on pore structure of cement mortar. *Constr. Build Mater.* **2013**, *38*, 804–812. [CrossRef]
50. Zhao, H.; Xiao, Q.; Huang, D.; Zhang, S. Influence of pore structure on compressive strength of cement mortar. *Sci. World J.* **2014**, *2014*. [CrossRef] [PubMed]
51. Berodier, E.; Scrivener, K. Evolution of pore structure in blended systems. *Cem. Concr. Res.* **2015**, *73*, 25–35. [CrossRef]
52. Dhandapani, Y.; Santhanam, M. Investigation on the microstructure-related characteristics to elucidate performance of composite cement with limestone-calcined clay combination. *Cem. Concr. Res.* **2020**, *129*, 105959. [CrossRef]
53. Ferreiro, S.; Herfort, D.; Damtoft, J.S. Effect of raw clay type, fineness, water-to-cement ratio and fly ash addition on workability and strength performance of calcined clay Limestone Portland cements. *Cem. Concr. Res.* **2017**, *101*, 1–12. [CrossRef]
54. Beaudoin, J.; Odler, I. Hydration, Setting and Hardening of Portland Cement. In *Lea's Chemistry of Cement and Concrete*, 5th ed.; Hewlett, P., Liska, M., Eds.; Elsevier: Amsterdam, The Netherlands, 2019; pp. 157–250.
55. Parashar, A.; Bishnoi, S. Hydration behaviour of limestone-calcined clay and limestone-slag blends in ternary cement. *RILEM Tech. Lett.* **2021**, *6*, 17–24. [CrossRef]
56. Zunino, F.; Scrivener, K. Microstructural developments of limestone calcined clay cement (LC3) pastes after long-term (3 years) hydration. *Cem. Concr. Res.* **2022**, *153*, 106693. [CrossRef]
57. Balshin, M.Y. Relation of mechanical properties of powder metals and their porosity and the ultimate properties of porous-metal ceramic materials. *Dokl. Akd. SSS* **1949**, *7*, 831–834.
58. Ryshkevitch, R. Compression strength of porous sintered alumina and zirconia. *J. Am. Ceram. Soc.* **1953**, *36*, 65–68. [CrossRef]
59. Schiller, K.K. Strength of porous materials. *Cem. Concr. Res.* **1971**, *1*, 419–422. [CrossRef]
60. Hasselman, D.P.H. Griffith flaws and the effect of porosity on tensile strength of brittle ceramics. *J. Am. Ceram. Soc.* **1969**, *52*, 457. [CrossRef]
61. Chen, X.; Wu, S.; Zhou, J. Influence of porosity on compressive and tensile strength of cement mortar. *Constr. Build Mater.* **2013**, *40*, 869–874. [CrossRef]
62. Wu, B.; Ye, G. Development of porosity of cement paste blended with supplementary cementitious materials after carbonation. *Constr. Build Mater* **2017**, *145*, 52–61. [CrossRef]
63. Favier, A.; Zunino, F.; Katrantzis, I.; Scrivener, K. The effect of limestone on the performance of ternary blended cement LC3: Limestone, Calcined Clays and Cement. In Proceedings of the 2nd International Conference on Calcined Clays for Sustainable Concrete, La Havana, Cuba, 5–7 December 2017. [CrossRef]